Carbohydrate Polymers 92 (2013) 1497–1502

Contents lists available at SciVerse ScienceDirect

Carbohydrate Polymers

journal homepage: www.elsevier.com/locate/carbpol

Removal of Remazol turquoise Blue G-133 from aqueous solution using modified waste newspaper fiber

Xiaoyu Zhang, Jia Tan, Xinhao Wei, Lijuan Wang*

Key Laboratory of Bio-based Material Science and Technology of Ministry of Education, Northeast Forestry University, 26 Hexing Road, Harbin 150040, PR China

ARTICLE INFO

Article history:
Received 11 March 2012
Received in revised form 26 August 2012
Accepted 26 October 2012
Available online 2 November 2012

Keywords:
Waste newspaper
Modification
Quaternary ammonium salt
Reactive dye
Adsorption mechanism

ABSTRACT

Waste newspaper fiber (WNF) was separated and modified via grafting quaternary ammonium salt to obtain an adsorbent, which removes Remazol turquoise Blue G-133 (RTB G-133) from aqueous solutions. SEM and IR were used to analyze the morphology and chemical groups of the modified waste newspaper fiber (MWNF). Batch adsorption studies were conducted with varying adsorbent dosages, solution pH, and contact time. Adsorption isotherms and models were fitted. The SEM photographs show the surface of MWNF is smoother in comparison with that of WNF. The IR analysis indicates that the quaternary ammonium salt was successfully grafted onto the cellulose skeleton in WNF and the chemical interaction played an important role in adsorption. Results show that the equilibrium adsorption capacity can be reached within 360 min, and that the maximum adsorption capacity was 260 mg g^{-1}. The adsorption of RTB G-133 on MWNF was a spontaneous endothermic process and well fitted pseudo-second-order kinetic model and Langmuir adsorption isotherm model. The results show that MWNF is promising for dye wastewater treatment.

1. Introduction

Various kinds of dyes are widely used in the textile, printing, plastic, and food industries (Altınışık, Gür, & Seki, 2010; Hameeda & El-Khaiary, 2008; Senturk, Ozdes, & Duran, 2010). Those industries produce large amount of colored effluents, which contain about 5–10% of dyestuff (Moussavi & Khosravi, 2011; Thangamani et al., 2007). Most modern dyes are synthesized and consist of toxic and carcinogenic compounds (Sun, Sun, Wang, & Qiao, 2007). Moreover, they are stable and very difficult to degrade in the wastewater effluent. Therefore, dye contamination of water causes severe environmental and public health problems.

It is urgent to develop various effective methods for the removal of dyes from wastewater because of strict legislation on the discharge of these toxic pollutants. Conventional methods such as coagulation-flocculation (Panswed & Wongchaisuwan, 1986; Szyguła, Guibal, Palacín, Ruiz, & Sastre, 2009; Verma, Roshan, & Bhunia, 2012), membrane filtration (Ciardelli, Corsi, & Marucci, 2000), chemical oxidation (Arslan & Balcioğlu, 1999; Arslan, Balcioğlu, & Bahnemann, 2000; Turgaya, Ersoza, Atalaya, Forssb, & Welanderb, 2011), and adsorption have been utilized for dye removal. Activated carbon is the most commonly used adsorbent for the treatment of dye effluents. Activated carbon itself is expensive and its regeneration adds to the high cost (Ali & Gupta, 2007; Garg, Amita, Kumar, & Gupta, 2004). Therefore, further development of adsorbents should be investigated. Research for cheaper and more effective adsorbents from agricultural residues and by-products have been done. These efforts have included pineapple stem, almond shell, jackfruit peel, orange peel (Vieira et al., 2009), sugarcane bagasse (Orlando, Okuda, & Nishijima, 2003), peanut hull (Gong, Ding, & Li, 2005), apple pomace (Robinson, Chandran, & Nigam, 2002), coconut husk (Manju, Raji, & Anirudhan, 1998), pine bark (Orlando et al., 2003) and meranti sawdust. Some of these materials have low adsorption capacity. However, they could be modified into higher performance absorbents for various pollutants (Xu, Gao, Yue, & Zhong, 2010).

Waste newspaper is an important form of domestic waste. The recycle of waste newspaper is necessary. Waste newspaper fiber (WNF) is a low-cost cellulosic material. Researchers have investigated the adsorption and porous properties of activated carbon from waste newspaper prepared by chemical and physical activation (Okada, Yamamoto, Kameshima, & Yasumori, 2003). WNF was directly used as a sorbent to absorb Cu (II) ion (Chakravarty, Pimple, Chaturvedi, Singh, & Gupta, 2008) and Cr (VI) ions (Wang & Li, 2009). Adsorption of zinc was studied using chemically modified WNF as an adsorbent in an aqueous medium (Chakravarty et al., 2007). However, the use of WNF for dye removal from aqueous effluents has not been previously investigated.

In the present study, a new sorbent based on WNF was developed via chemical modification in which quaternary ammonium

* Corresponding author.
E-mail address: donglinwlj@163.com (L. Wang).

0144-8617/$ – see front matter.
http://dx.doi.org/10.1016/j.carbpol.2012.10.066

cationic groups were introduced into the cellulose backbone of WNF. The modified waste newspaper fibers (MWNFs) bearing quaternary ammonium cationic groups were characterized and then used as a sorbent for the removal of RTB G-133 anionic dye from aqueous solutions at various experimental conditions. Kinetic and isotherm parameters were also investigated.

2. Materials and methods

2.1. Separation and pretreatment of WNF

Waste newspaper was cut into small pieces and soaked in tap water for about 2 days. The fibers were obtained after being sorted and screened in the beater. The WNF was treated with an aqueous solution containing 1.5% NaOH, 3.0% H_2O_2, 0.3% Na_2SiO_3 and 1.5% surfactant for removing black ink. After processing, WNF was washed several times with distilled water until the supernatant pH was 6.5–7.0. The pretreated WNF was dried to a constant weight in an oven at 103 °C. Then, the dry WNF was ground to a powder of 80–120 mesh size for further use. The chemical composition of WNF was analyzed and the results are as follows: moisture content 4.26%, extractive 0.95%, holocellulose 82.44%, lignin 12.35%, and pentosan 8.61%. The main component of WNF is cellulose, with a content of 73.83%.

2.2. The preparation of MWNF

A 10 g sample of WNF powder and 250 mL of 10% NaOH were added into the three-neck round bottom flask and agitated for 1 h at room temperature. Then half of the solution was removed and immediately 50 mL of distilled water and 80 mL epoxy chloropropane were added. The mixture was heated in a 65 °C water bath and stirred for 6 h. After which, the solution was removed from the heat and 110 mL of 34% triethylamine solution (w/w) was added. The mixture was heated in a 80 °C water bath and agitated for 3 h. The product was washed sequentially with ethanol and distilled water. The solution pH was then adjusted around 7 using 0.1 M NaOH and 0.1 M HCl. Finally, the product was cleaned with distilled water until the pH was around 7. The MWNF was dried at 60 °C for 12 h.

2.3. Characterization of the MWNF

FTIR spectra were recorded using a Nicolet 560 spectrometer (Nicolet Co., USA) at a resolution of 4 cm and using the KBr pellet method. Morphological analysis was conducted with a Quanta 200 device (Philips-FEI Co., Netherlands). The scanned surfaces were coated with a thin layer of gold before observation. Surface area and pore volume of the WNF and MWNF were calculated by means of the nitrogen adsorption isotherm at 77 K through the ASAP 2010 analyzer (Micometrics, USA). The point of zero charge (pH_{PZC}) was determined by the solid addition method (Vieira et al., 2009). To a series of 100 mL conical flasks, 10.0 mL of NaCl solution were transferred with pH ranging between 2 and 11. Then, 0.05 g of MWNF was added to each flask, which was securely capped immediately and shaken for 10 h. The difference between the final and initial pH value (ΔpH) was plotted against the initial pH and the point of intersection on X axis corresponds to the point zero charge (pH_{PZC}). The same measurements for WNF were conducted. The nitrogen content of MWNF was determined using a K-Alpha XPS Analyzer (ThermoFisher Scientific Company). The quantitative XPS results can be used to estimate the degree hydroxyl groups of substitution (DS) and the formula can be seen in Ref. (Alila, Ferraria, Rego, & Boufi, 2009).

2.4. Preparation of dye solution

Remazol Turquoise Blue G 133 (C.I. Reactive Blue 21, λ_{max} 660 nm) was supplied by DyStar (Shanghai) Trading Co., Ltd. It is a copper phthalocyanine with a sulfato ethyl sulfone as reactive group. An accurate weighed quantity of the dye was dissolved in distilled water to prepare a 100 mg L^{-1} stock solution. Experimental solutions of various concentrations were created by further dilutions. Standard curves were made using the absorbance measurement of the dye solution by UV–visible spectrophotometer (TU-1900).

3. Experimental

3.1. Adsorption experiment

Batch sorption experiments were conducted to evaluate the effects of various parameters such as pH, adsorbent dose, initial dye concentration, and contact time on the adsorption of Remazol Turqueise Blue G-133 (RTB G-133). In each adsorption experiment, 100 mL of dye solution was added to the amount of adsorbent in a 250 mL of conical flask at room temperature, and the mixture was shaken at 190 rpm in a water bath oscillator.

The sample was withdrawn from the oscillator at the end of the adsorption, and the adsorbents were separated from the solution with a 400-mesh pore size, nylon screen. The absorbance of the residue solution was measured to calculate the dye concentration.

The dye removal efficiency (R), the amount of absorbed dye per unit mass of sorbent at moment t (q_t, mg g^{-1}) and at equilibrium (q_e, mg g^{-1}) were calculated by using the following equations:

$$R(\%) = \frac{C_0 - C_t}{C_0} \times 100\% \quad (1)$$

$$q_t = \frac{(C_0 - C_t)V}{W} \quad (2)$$

$$q_e = \frac{(C_0 - C_e)V}{W} \quad (3)$$

where C_t (mg L^{-1}) is the dye concentration at time t. C_0 and C_e (mg L^{-1}) are the initial and equilibrium concentrations of dye solution, respectively. V is the volume of dye solution (mL) and W is the amount of the adsorbent (g).

The effect of pH on the adsorption of RTB G-133 by MWNF was determined using different pH values (2–10) by adding a few drops of NaOH or HCl solution.

3.2. Kinetic studies

The kinetics of adsorption was determined by analyzing the dye absorbed from aqueous solution at different time intervals. Initial dye concentrations in the test solution and adsorbent dosage were varied to investigate their effects on the adsorption kinetics.

4. Results and discussion

4.1. Characterization

The FTIR spectra of WNF and MWNF are shown in Fig. 1. In Fig. 1(a), the band at 3400 cm^{-1} is attributed to stretching of —OH group. The peak at 2903 cm^{-1} corresponds to C—H stretching. The band at 1513 cm^{-1} corresponds to aromatic ring vibrations of the phenylpropane skeleton. The peaks at 1270 cm^{-1} and 810 cm^{-1} are attributed to C—O stretching of guaiacyl rings. A series of peaks at

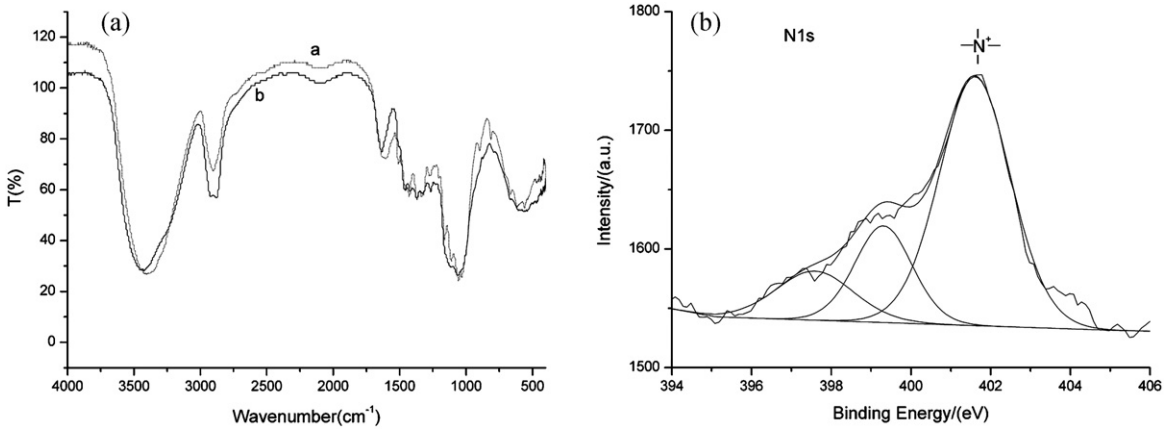

Fig. 1. Characterization of MWNF: (a) FT-IR spectra of (a) WNF and (b) MWNF, (b) N 1s spectrum.

1033 cm^{-1}, 1061 cm^{-1}, 1115 cm^{-1}, and 1165 cm^{-1} correspond to —C—O—C— bonds in the anhydroglucose unit in cellulose. In contrast to WNF, the bands at 1513 cm^{-1} and 810 cm^{-1} disappeared, and the peak at 3400 cm^{-1} shifted to 3441 cm^{-1}. Moreover, the peak at 2900 cm^{-1} became stronger and a shoulder peak occurred. These peaks indicate that NaOH treatment in the first stage of the synthesis process further removed some soluble lignin in WNF. Epoxy chloropropane introduced new $—CH_2$ groups to the cellulose molecule. There is a new adsorption peak associated with the stretching vibration of C—N band at 1465 cm^{-1}, and a broad band of the skeletal vibration of the quaternary ammonium salt, which was successfully grafted onto the cellulose skeleton (Cao et al., 2011). As shown in Fig. 1(b), the peaks at 401.6 eV in the XPS spectrum further proved that MWNF contains nitrogen in quaternary state (Tastet et al., 2011). The obtained DS value of quaternary ammonium group was 0.22.

SEM photographs of WNF and MWNF were obtained at an amplified of 5000×, shown in Fig. 2. It is clearly seen in Fig. 2(a) that the surface of WNF is coarse and rough. As shown in Fig. 2(b), the prepared MWNF appears to have a smoother surface with homogenous creases.

The result for BET surface area and the total pore volume for WNF and MWNF were 2.36 $m^2\,g^{-1}$ and 0.0033 $cm^3\,g^{-1}$, and 1.30 $m^2\,g^{-1}$ and 0.0003 $cm^3\,g^{-1}$, respectively. All those indicate that the modification changed the surface of WNF and MWNF contains mesoporous structure. The BET surface area is low in comparison with those of porous sorbents (BET surface area range from 500 $m^2\,g^{-1}$ to 2500 $m^2\,g^{-1}$), which indicates that the absence of pore adsorption in the sorption process.

4.2. Effect of adsorbent dose

The effect of sorbent dosage on adsorption of RTB G-133 is shown in Fig. 3(a). The adsorption capacity of dye decreased with the increasing dosage of MWNF. The sorbents are not fully utilized because of the increase in available sorption sites with increasing MWNF dosage. As shown in Fig. 3(b), the removal of RTB G-133 increased with the increase in MWNF dosage and the solution became colorless when dosage exceeded 0.03 g.

4.3. Effect of initial pH

The pH of the solution is a key factor in the adsorption process. Several parameters such as adsorption capacity of adsorbent, surface charges, active sites and chemistry of the dye might be attributed to the adsorption behavior under various pH values. The pH_{PZC} of MWNF is around 8.1. Theoretically, when the pH is lower than 8.1, the MWNF surface becomes positively charged, which favors the adsorption of the negatively charged dye anions via electrostatic attraction. Certainly, for pH > 8.1, the surface becomes deprotonated, which stops the attraction of dye anions. However, the adsorption behavior did not follow the theoretical prediction. The original pH of RTB G133 solution is 5.75. Fig. 4 presents the practical effect of pH on dye sorption on MWNF. RTB G-133 is a reactive dyestuff, which contains $—SO_3H$ group in the molecule. Under strongly acid conditions, the $—SO_3H$ group can react with quaternary ammonium group to form cell $—R—N^+(C_2H_5)_3\cdots SO_3^-$. As the pH increases, the $—SO_3H$ group are reduced, resulting in the decrease of interaction between the dye molecules and MWNF.

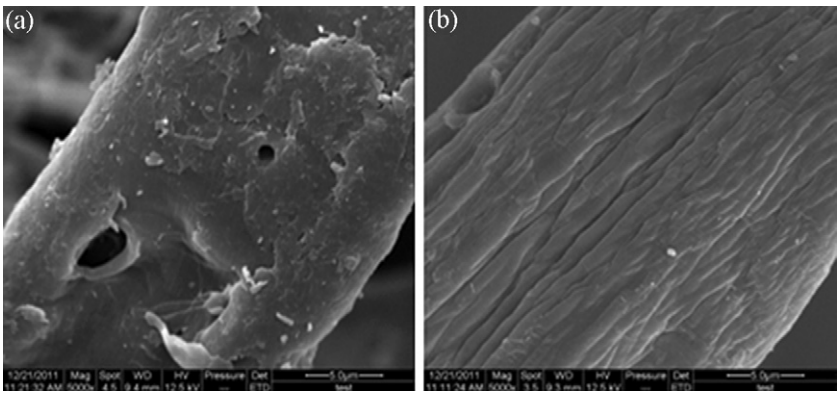

Fig. 2. SEM photographs of WNF (a) and MWNF (b).

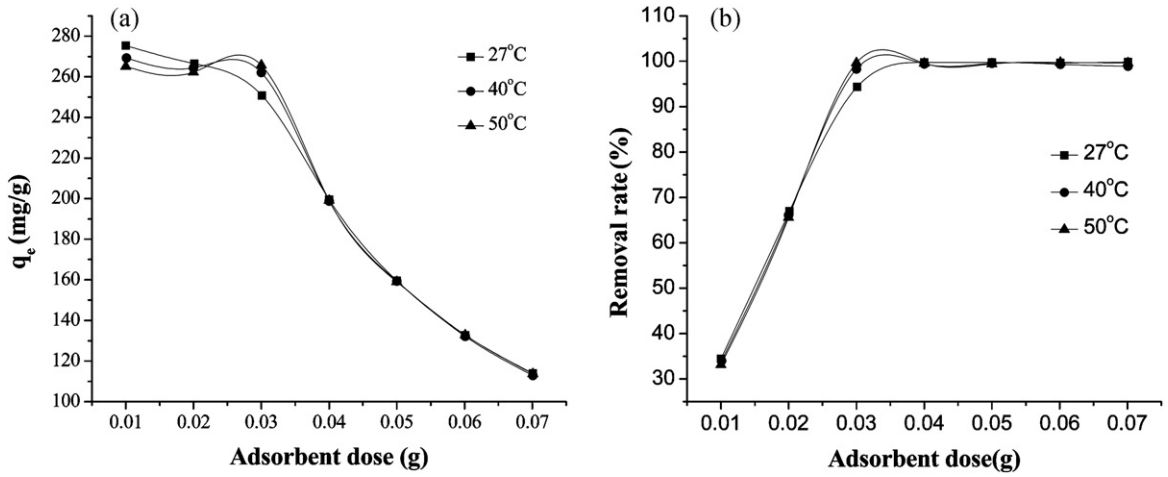

Fig. 3. Effect of adsorbent dose on the adsorption (a) and (b) of RTB G 133 (initial pH, t = 10 h, C = 80 mg L^{-1}, and V = 100 mL).

Moreover, more OH^- ions will compete for the sorption sites on sorbent with dye molecules with increasing pH, which results in a decrease of adsorption capacity. However, RTB G133 is sensitive to pH, therefore, higher pH may result in molecule aggregation, which is favorable to the adsorption. The results in Fig. 4 are from the joint action of the two opposite trends, especially, in alkaline pH. The maximum adsorption capacity of 260 mg g^{-1} can be obtained under pH 2.

4.4. Effect of contact time

The effects of contact time on the adsorption of RTB G-133 onto MWNF are shown in Fig. 5. It indicates that the adsorption capacity increases with increasing contact time. The fastest rate of change in absorption capacity occurs during and the first 60 min. The equilibrium time varies with sorption temperature. At higher temperatures, the equilibrium time is shorter. The results show that the contact times needed for RTB G-133 at 33 °C, 40 °C, and 50 °C are 360 min, 360 min and 180 min, respectively. Therefore, improving the temperature can accelerate the adsorption equilibrium.

4.5. Sorption kinetics

The study of kinetics is important to optimize different operating parameters for the sorption process. Two kinetic models have been suggested to explain the order of the adsorption.

The kinetics of RTB G-133 sorption onto MWNF was analyzed using pseudo-first order and pseudo-second order kinetic models.

The pseudo-first order kinetic model (Ahmad, Hameed, & Aziz, 2007; Hamdaoui, Saoudi, Chiha, & Naffrechoux, 2008) can be expressed as follows:

$$\ln(q_e - q_t) = \ln\ q_e - k_1 t \tag{4}$$

where q_e and q_t are the adsorption capacity (mg g^{-1}) at equilibrium e and time t, respectively. k_1 is the rate constant (L min^{-1}) of the pseudo-first order kinetic model.

The pseudo-second order kinetic model (Kumar & Sivanesan, 2007) can be expressed as Eq. (5):

$$\frac{t}{q_t} = \frac{1}{k_2 q_e^2} + \frac{t}{q_e} \tag{5}$$

where k_2 (g mg^{-1} min^{-1}) is the rate constant for the pseudo-second order kinetic model. The q_e and k_2 values were estimated from the slope ($1/q_e$) and intercept ($1/k_2 q_e^2$) of a linear plot of t/q_t versus t at different dye concentrations.

Straight-line plots of $\log(q_e - q_t)$ against time (Eq. (4)) were made at different dye concentrations, as shown in Fig. 5.

The kinetic parameters at different temperatures are calculated and shown in Fig. 6 and Table 1. The results show that the Pseudo-second-order kinetic model describes the whole sorption process. The $q_{e,calc}$ and $q_{e,exp}$ of pseudo-second-order are very close and all the values of R^2 were higher than 0.999, which showed that the

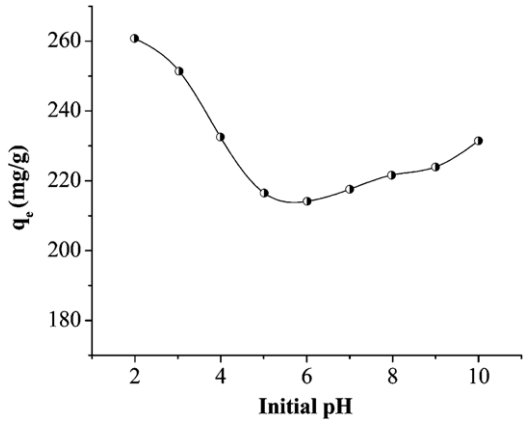

Fig. 4. Effect of pH on the adsorption of RTB G-133 (dosage 30 mg, T = 28.7 °C, t = 3 h, C = 80 mg L^{-1}, and V = 100 mL).

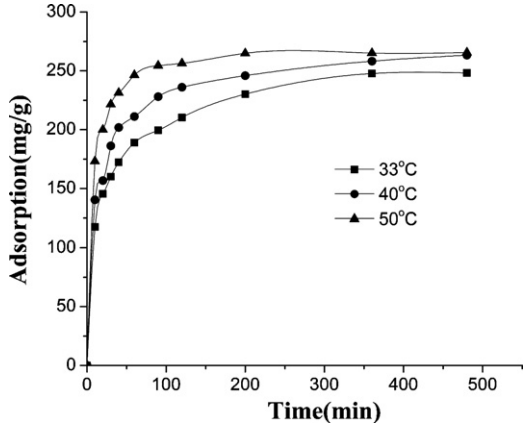

Fig. 5. Effect of contact time on the adsorption of RTB G 133(dosage 30 mg, pH = 5, C = 80 mg L^{-1}, and V = 100 mL).

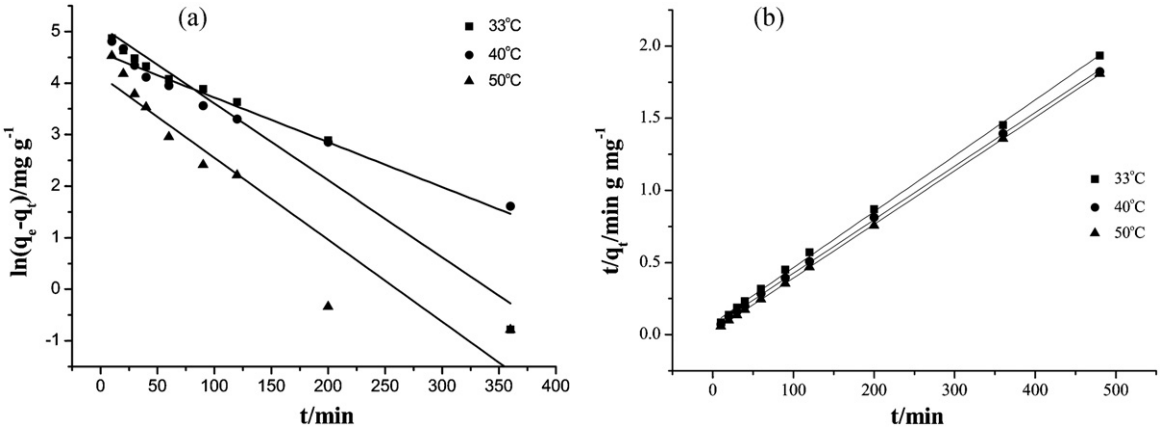

Fig. 6. Kinetics models of (a) pseudo-first-order and (b) pseudo-second-order.

Table 1
Kinetic parameters for sorption of RTB G-133 on MWNF.

T (°C)	$q_{e,exp}$ (mg g^{-1})	Pseudo-first-order			Pseudo-second-order		
		k_1 (min^{-1})	$q_{e,calc}$ (mg g^{-1})	R^2	k_2 (mg g^{-1} min^{-1})	$q_{e,calc}$ (mg g^{-1})	R^2
33	248.17	0.015	164.28	0.954	1.95	257.73	0.999
40	263.24	0.009	98.35	0.959	2.54	269.54	0.999
50	265.55	0.016	62.87	0.899	6.32	269.54	1.000

adsorption of RTB G-133 on MWNF accurately followed the pseudo-second order kinetic model. The R^2 values of were satisfactory in the pseudo-first-order model. However, the value of $q_{e,calc}$ was only about half that of $q_{e,exp}$. Therefore, the adsorption did not fit the pseudo-first order kinetic model well.

4.6. Sorption isotherms

Several models have been used to describe experimental data of adsorption isotherms. The Langmuir (Li, Gao, Wu, Wang, & Li, 2009) and Freundlich (1906) are the most often-used models. These models are represented mathematically as follows:

Langmuir equation:

$$\frac{C_e}{q_e} = \frac{1}{bq_m} + \frac{C_e}{q_m} \tag{6}$$

Freundlich equation:

$$\log q_e = \log k_f + \left(\frac{1}{n}\right) \log C_e \tag{7}$$

where q_e (mg g^{-1}) is the equilibrium adsorption capacity of the sorbent, C_e (mg L^{-1}) is the equilibrium concentration of the dye solution absorbed; q_m (mg g^{-1}), the maximum monolayer capacity of the sorbent; and b (L mg^{-1}) is a Langmuir isotherm constant. K_f is the Freundlich constant, and $1/n$ is the heterogeneity factor. Table 2 shows the calculated parameters for Langmuir and Freundich isotherms models for RTB G-133 on MWNF. R^2 values of the Langmuir isotherms are uniform and higher than 0.998, however, Freundlich isotherms are lower, indicating that the adsorption of RTB G-133 on MWNF obeyed the Langmuir model well compared with Freundlich isotherms. This result suggests that the uptake of RTB G-133 occurs on the homogeneous surface of MWNF by monolayer adsorption without interaction between the absorbed RTB G-133 molecules.

Table 2
Isotherm parameters for sorption of RTB G 133 on MWNF.

Temperature (°C)	Langmuir isotherm			Freundlich isotherm		
	b (L mg^{-1})	q_m (mg g^{-1})	R^2	K_f (L g^{-1})	n	R^2
28	0.214	315.46	0.999	165.55	7.2	0.984
40	0.497	305.81	0.998	230.36	16.8	0.928
50	1.186	296.74	0.998	267.71	51.5	0.734

The maximum adsorption capacity of RTB G-133 on various sorbent was compared. In comparison with other materials, the maximum adsorption capacity of RTB G-133 on MWNF is higher than those in previous studies, such as 106.71 mg g^{-1} of fly ash and 106.71 mg g^{-1} of sepiolite (Demirbas & Nas, 2009), 92.2 mg g^{-1} of dried *Rhizopus arrhizus* (Aksu & Çağgatay, 2006), 83.7 mg g^{-1} of agricultural waste sugar beet pulp (Aksu & Isoglu, 2006), and 45.7 mg g^{-1} of immobilized *Scendesmus* (Ergene, Ada, Tan, & Katırcıoğlu, 2009). In our laboratory, we also measured the adsorption capacity of RTB G-133 on commercial activated carbon. It is about 160 mg g^{-1} and 100 mg g^{-1} lower than that of MWNF. The comparison indicates that MWNF has potential for dye removal from wastewater.

4.7. Sorption thermodynamic

In the practice, thermodynamic parameters are extremely important and must be taken into consideration to evaluate the spontaneity of the adsorption process. The thermodynamic parameters such as enthalpy change (ΔH°), free energy change (ΔG°) and entropy change (ΔS°) were calculated from the sorption of RTB G-133 on MWNF temperature data (Buvaneswari & Kannan, 2011).

According to the Van't Hoff equation:

$$\Delta G^\circ = \Delta H^\circ - T\Delta S^\circ = -RT \ln k_c \tag{8}$$

$$k_c = \frac{C_s}{C_e} \tag{9}$$

$$\ln k_c = -\left(\frac{\Delta H^\circ}{RT}\right) + \frac{\Delta S^\circ}{R} \tag{10}$$

The values of ΔG° and ΔH° were obtained from the slope and intercept of the Van't Hoff curve. The thermodynamic parameters as follows: ΔH° 216.62 kJ mol^{-1}, ΔS° 738.68 J mol^{-1} K^{-1}, and ΔG° −9.53 kJ mol^{-1}, −14.70 kJ mol^{-1}, −22.09 kJ mol^{-1} at 33 °C, 40 °C, and 50 °C, respectively. The negative value of ΔG° indicates that

the spontaneity and feasibility of the sorption of RTB G-133 on the sorbent. The positive value of ΔH° reflects that the sorption is endothermic in nature. The positive value of ΔS° shows that the increase in randomness at the interface during the sorption process. The results indicate that the adsorption capacity increases with the increasing temperature.

5. Conclusions

MWNF is an effective sorbent for the removal of RTB G-133 from aqueous media. Low initial pH and high temperature of the dye solution favors sorption. The adsorption capacity can reach 260 mg g^{-1}. The adsorption followed the pseudo-second-order kinetic model well. The Langmuir isotherm provided the highest correlation of the experimental data for RTB G-133. Thermodynamic studies showed that the sorption was spontaneous and endothermic process. The study indicates that MWNF could be utilized to prevent environmental pollution.

Acknowledgments

The authors gratefully acknowledge Fundamental Research Funds for the Central Universities (DL12DB04) and Innovation Experiment Program for University Students in NEFU (1110225029).

References

Ahmad, A. A., Hameed, B. H., & Aziz, N. (2007). Adsorption of direct dye on palm ash: Kinetic and equilibrium modeling. *Journal of Hazardous Materials*, *141*, 70–76.

Aksu, Z., & Çağgatay, Ş. Ş. (2006). Investigation of biosorption of Gemazol Turquise Blue-G reactive dye by dried *Rhizopus arrhizus* in batch and continuous systems. *Separation and Purification Technology*, *48*, 24–35.

Aksu, Z., & Isoglu, I. A. (2006). Use of agricultural waste sugar beet pulp for the removal of Gemazol turquoise blue-G reactive dye from aqueous solution. *Journal of Hazardous Materials*, *B137*, 418–430.

Ali, I., & Gupta, V. K. (2007). Advances in water treatment by adsorption technology. *Nature Protocols*, *1*, 2661–2667.

Alila, S., Ferraria, A. M., Rego, A. M. B., & Boufi, S. (2009). Controlled surface modification of cellulose fiber by amino derivatives using N,N′-carbonyldiimidazole as activator. *Carbohydrate Polymers*, *77*, 553–562.

Altınışık, A., Gür, E., & Seki, Y. (2010). A natural sorbent, *Luffa cylindrica* for the removal of a model basic dye. *Journal of Hazardous Materials*, *179*, 658–664.

Arslan, I., & Balcioğlu, I. A. (1999). Degradation of commercial reactive dyestuffs by heterogenous and homogenous advanced oxidation processes: A comparative study. *Dyes and Pigments*, *43*, 95–108.

Arslan, İ, Balcioğlu, I. A., & Bahnemann, D. W. (2000). Advanced chemical oxidation of reactive dyes in simulated dyehouse effluents by ferrioxalate-Fenton/UV-A and TiO_2/UV-A processes. *Dyes and Pigments*, *47*, 207–218.

Buvaneswari, N., & Kannan, C. (2011). Plant toxic and non-toxic nature of organic dyes through adsorption mechanism on cellulose surface. *Journal of Hazardous Materials*, *189*, 294–300.

Cao, W., Dang, Z., Zhou, X., Yi, X., Wu, P., Zhu, C., et al. (2011). Removal of sulphate from aqueous solution using modified rice straw: Preparation, characterization and adsorption performance. *Carbohydrate Polymer*, *85*, 571–577.

Chakravarty, S., Bhattacharjee, S., Gupta, K. K., Singh, M., Chaturvedi, H. T., & Maity, S. (2007). Adsorption of zinc from aqueous solution using chemically treated newspaper pulp. *Bioresource Technology*, *98*, 3136–3141.

Chakravarty, S., Pimple, S., Chaturvedi, H. T., Singh, S., & Gupta, K. K. (2008). Removal of copper from aqueous solution using newspaper pulp as an adsorbent. *Journal of Hazardous Materials*, *159*, 396–403.

Ciardelli, G., Corsi, L., & Marucci, M. (2000). Membrane separation for wastewater reuse in the textile industry. *Resources, Conservation and Recycling*, *31*, 189–197.

Demirbas, E., & Nas, M. Z. (2009). Batch kinetic and equilibrium studies of adsorption of Reactive Blue 21 by fly ash and sepiolite. *Desalination*, *243*, 8–21.

Ergene, A., Ada, K., Tan, S., & Katırcıoğlu, H. (2009).Removal of Remazol Brilliant Blue R dye from aqueous solutions by adsorption onto immobilized *Scenedesmus quadricauda*: Equilibrium and kinetic modeling studies. *Desalination*, *249*, 1308–1314.

Freundlich, H. M. F. (1906). Over the adsorption in solution. *Journal of Physical and Chemistry*, *57*, 385–470.

Garg, V. K., Amita, M., Kumar, R., & Gupta, R. (2004). Basic dyes (methylene blue) removal from simulated wastewater by adsorption using Indian Rosewood sawdust: A timber industry waste. *Dyes and Pigments*, *63*, 243–250.

Gong, R. M., Ding, Y., & Li, M. (2005). Utilization of powdered peanut hull as biosorbent for removal of anionic dyes from aqueous solution. *Dyes and Pigments*, *64*, 187–192.

Hamdaoui, O., Saoudi, F., Chiha, M., & Naffrechoux, E. (2008). Sorption of malachite green by a novel sorbent, dead leaves of plane tree: Equilibrium and kinetic modeling. *Chemical Engineering Journal*, *143*, 73–84.

Hameeda, B. H., & El-Khaiary, M. I. (2008). Malachite green adsorption by rattan sawdust: Isotherm, kinetic and mechanism modeling. *Journal of Hazardous Materials*, *159*, 574–579.

Kumar, K. V., & Sivanesan, S. (2007). Isotherms for malachite green onto rubber wood (*Hevea brasiliensis*) sawdust: Comparison of linear and non-linear methods. *Dyes and Pigments*, *72*, 124–129.

Li, Y., Gao, B., Wu, T., Wang, B., & Li, X. (2009). Adsorption properties of aluminum magnesium mixed hydroxide for the model anionic dye reactive brilliant red K-2BP. *Journal of Hazardous Materials*, *164*, 1098–1104.

Manju, G. N., Raji, C., & Anirudhan, T. S. (1998). Evaluation of coconut husk carbon for the removal of arsenic from water. *Water Research*, *32*, 3062–3070.

Moussavi, G., & Khosravi, R. (2011). The removal of cationic dyes from aqueous solutions by adsorption onto pistachio hull waste. *Chemical Engineering Research and Design*, *89*, 2182–2189.

Okada, K., Yamamoto, N., Kameshima, Y., & Yasumori, A. (2003). Adsorption properties of activated carbon from waste newspaper prepared by chemical and physical activation. *Journal of Colloid and Interface Science*, *262*, 194–199.

Orlando, U. S., Okuda, T., & Nishijima, W. (2003). Chemical properties of anion exchangers prepared from waste natural materials. *Reactive and Functional Polymers*, *55*, 311–318.

Panswed, J., & Wongchaisuwan, S. (1986). Mechanism of dye wastewater color removal by magnesium carbonate-hydrated basic. *Water Science and Technology*, *18*, 139–144.

Robinson, T., Chandran, B., & Nigam, P. (2002). Removal of dyes from a synthetic textile dye effluent by biosorption on apple pomace and wheat straw. *Water Research*, *36*, 2824–2830.

Senturk, H. B., Ozdes, D., & Duran, C. (2010). Biosorption of Rhodamine 6G from aqueous solutions onto almond shell (*Prunus dulcis*) as a low cost biosorbent. *Desalination*, *252*, 81–87.

Sun, J., Sun, S., Wang, G., & Qiao, L. (2007). Degradation of azo dye Amido black 10B in aqueous solutions by Fenton oxidation process. *Dyes and Pigments*, *74*, 647–652.

Szyguła, A., Guibal, E., Palacín, M. A., Ruiz, M., & Sastre, A. M. (2009). Removal of an anionic dye (Acid Blue 92) by coagulation–flocculation using chitosan. *Journal of Environmental Management*, *90*, 2979–2986.

Tastet, D., Save, M., Charrier, F., Charrier, B., Ledeuil, J. B., Dupin, J. C., et al. (2011). Functional biohybrid materials synthesized via surface-initiated MADIX/RAFT polymerization from renewable natural wood fiber: Grafting of polymer as non leaching preservative. *Polymer*, *52*, 606–616.

Thangamani, K. S., Sathishkumar, M., Sameena, Y., Vennilamani, N., Kadirvelu, K., Pattabhi, S., et al. (2007). Utilization of modiWed silk cotton hull waste as an adsorbent for the removal of textile dye (reactive blue MR) from aqueous solution. *Bioresource Technology*, *98*, 1265–1269.

Turgaya, O., Ersoza, G., Atalaya, S., Forssb, J., & Welanderb, U. (2011). The treatment of azo dyes found in textile industry wastewater by anaerobic biological method and chemical oxidation. *Separation and Purification Technology*, *79*, 26–33.

Verma, A. K., Roshan, D. R., & Bhunia, P. (2012). A review on chemical coagulation/flocculation technologies for removal of colour from textile wastewaters. *Journal of Environmental Management*, *93*, 154–168.

Vieira, A. P., Santana, S. A. A., Bezerra, C. W. B., Silva, H. A. S., Chaves, J. A. P., Melo, J. C. P., et al. (2009). Kinetics and thermodynamics of textile dye adsorption from aqueous solutions using babassu coconut mesocarp. *Journal of Hazardous Materials*, *166*, 1272–1278.

Wang, X., & Li, Z. (2009). Removal of Cr (VI) from aqueous solution by newspapers. *Desalination*, *249*, 175–181.

Xu, X., Gao, B., Yue, Q., & Zhong, Q. (2010). Preparation of agricultural by-product based anion exchanger and its utilization for nitrate and phosphate removal. *Bioresource Technology*, *101*, 8558–8564.